Published in final edited form as:
Immunol Invest. 2014 ; 43(3): 255–266. doi:10.3109/08820139.2013.864667.

Pro-inflammatory effects of uric acid in the gastrointestinal tract

John K. Crane and **Krystin M. Mongiardo**
Deparment of Medicine, Division of Infectious Diseases, University at Buffalo, Buffalo, New York, USA

Abstract

Uric acid can be generated in the gastrointestinal (GI) tract from the breakdown of nucleotides ingested in the diet or from purines released from host cells as a result of pathogen-induced cell damage. Xanthine oxidase (XO) is the enzyme that converts hypoxanthine or xanthine into uric acid, a reaction that also generates hydrogen peroxide. It has been assumed that the product of XO responsible for the pro-inflammatory effects of this enzyme is hydrogen peroxide. Recent literature on uric acid, however, has indicated that uric acid itself may have biological effects. We tested whether uric acid itself has detectable pro-inflammatory effects using an in vivo model using ligated rabbit intestinal segments ("loops") as well as in vitro assays using cultured cells. Addition of exogenous uric acid increased the influx of heterophils into rabbit intestinal loops, as measured by myeloperoxidase activity. In addition, white blood cells adhered avidly to uric acid crystals, forming large aggregates of cells. Uric acid acts as a leukocyte chemoattractant in the GI tract. The role of uric acid in enteric infections and in non-infectious disorders of the GI tract deserves more attention.

Keywords

Birefringence; crystals; enteropathogenic; gout of the gut; shiga toxin; xanthine oxidase

INTRODUCTION

Xanthine oxidase (XO), also known as xanthine oxidoreductase, has been long recognized as an important host defense molecule in the gastrointestinal tract, liver, and in milk (Hancock et al., 2002; Harrison, 2006; Martin et al., 2004). We recently reported that XO activity is released into the lumen of the gut in response to infection with enteropathogenic *E. coli* (EPEC) and Shiga-toxigenic *E. coli* (STEC) in vivo. EPEC is a cause of prolonged watery diarrhea in children in developing countries (Kotloff et al., 2013), while STEC is the most common cause of "*E. coli* outbreaks" widely reported in the news media in developed countries (Frank et al., 2011). Because XO produces hydrogen peroxide, a strong oxidant, it has been natural to assume that most or all of the pro-inflammatory effects of XO activity are due to the peroxide.

The other main product of XO activity, however, is uric acid. In the last several years uric acid has been recognized to have a significant signaling role in innate immunity. Uric acid belongs to the damage-associated molecular pattern (DAMP) group of molecules and is

Correspondence: John K. Crane, Division of Infectious Diseases, Room 317, Biomedical Research Bldg., 3435 Main St., Buffalo, NY 14214, USA. jcrane@buffalo.edu.

DECLARATION OF INTEREST
The authors report no conflict of interest. The authors alone are responsible for the content and writing of the paper.

recognized as a “danger signal” to the immune system (Behrens et al., 2008; Bianchi, 2007; Heath & Carbone, 2003; Shi et al., 2003). In several experimental systems, formation of uric acid crystals, more accurately known as monosodium urate crystals, are required for maximal signaling in innate immunity.

In this study we examined whether sodium urate crystals are formed in vivo in the lumen of the gut in response to infection, and whether uric acid, as opposed to hydrogen peroxide, has detectable biological effects. Here, we use the term “uric acid crystals” instead of the more chemically accurate name monosodium urate (MSU) crystals, since the former term is already deeply entrenched in the biomedical literature (Howard et al., 2011) and familiar to many readers.

We found that uric acid crystals were formed in vivo in the lumen of the gut during infection with EPEC in the rabbit intestinal loop model of infection. We further found that uric acid crystals had pro-inflammatory effects independent of hydrogen peroxide.

METHODS

Reagents

Uricase enzyme was from Worthington Biochemicals, Freehold, NJ. Xanthine oxidase (XO), adenosine deaminase, uric acid and hypoxanthine were from Sigma-Aldrich, St. Louis, MO. Erythro-hydroxy-nonyl-adenine (EHNA) was from Calbiochem, now EMD Biosciences, Darmstadt, Germany.

Rabbit Infection Experiments Using Ligated Intestinal Loops

Animal experiments were approved by the IACUC of the Univ. at Buffalo. The 10-cm lengths of ileum were tied into segments (“loops”) as previously described (Crane et al., 2007) and injected with uric acid alone, uricase alone, or both. Loop contents were collected after 20 h. Wild-type rabbit EPEC strain E22, serotype O103:H4, was used as the infecting strain in Figure 1 and has been previously described (Milon et al., 1999).

Uric Acid Assay

Uric acid was measured using Quantichrom Uric Acid kits from Bioassay Systems (Hayward, CA). Following the manufacturers’ instructions, samples were subjected to filtration using 10 000 molecular weight cut-off filters (Corning Spin-X UF 10 K MWCO) in an Eppendorf microcentrifuge in order to remove interfering substances such as hemoglobin prior to uric acid determination, as previously described (Crane et al., 2007).

Myeloperoxidase Assay

Myeloperoxidase (MPO), a marker of neutrophils and of the equivalent polymorphonuclear leukocyte in the rabbit, heterophils, was measured using a fluorescent MPO assay kit from Cell Technology Inc., Mountain View, CA, following the manufacturer’s instructions. Rabbit loop fluids were clarified by centrifugation at 13 000 g × 10 min to remove cells and debris prior to assay. The supernatants were treated with N-ethylmaleimide (NEM) to inactivate glutathione according to the kit instructions, but the optional eosinophil inhibitor and the catalase inhibitor were not added.

Detection of Uric Acid Crystals by Birefringence Using Polarization Microscopy

We looked for uric acid crystals in the light microscope using two polarizing filters, one placed below the specimen (“polarizer”) and the other above the specimen (“analyzer”). By rotating the analyzer to a position where the plane of polarization is 90 degrees relative to

the polarizer, the field becomes dark. Crystals which rotate the plane of polarized light show up as bright objects on a midnight-blue field, known as birefringence. In order to practice and optimize the technique, calcite crystals (calcium carbonate crystals) were used as a positive control.

Microscopy was with a Nikon Optiphot 2 microscope equipped with a Retiga2000 digital camera. Images were acquired using the program ImageCapture Plus for the MacIntosh from Qimaging, the maker of the camera. In order to determine if the crystals we observed were negatively or positively birefringent, we used the first order red plate method to determine the refractive index in the gamma direction versus the alpha direction. Birefringence by this method was negative, i.e., $n_\gamma - n_\alpha < 0$.

Interaction of Uric Acid Crystals with Leukocytes

HL-60 cells, an acute promyelocytic leukemia cell line, were used to determine if uric acid crystals had leukoattractant or leukoagglutinating ability. HL-60 cells were purchased from the American Type Culture Collection (ATCC, Manassas, VA) and grown as previously described (Crane et al., 1999). Uric acid is not very soluble, even in solvents such as DMSO, meaning that concentrations of DMSO as high as 5% are carried over when uric acid is added in sufficient quantity to trigger precipitation. To circumvent the problem of low uric acid solubility, we created uric acid in vitro by adding hypoxanthine plus 0.5 U/mL XO. To some conditions we also added 600 U/mL catalase to break down hydrogen peroxide (Figure 3, Panels B and C) and to some we added 2 U/mL uricase to remove uric acid as it was formed.

Experiments with Rabbit Peripheral Blood Leukocytes (PBLs)

First, 10 mL of blood was drawn by ear vein and collected in heparinized tubes. Blood was diluted 6-fold into PBS + heparin, then PBLs were isolated using ammonium chloride lysis to remove red blood cells as described by Tait et al. (1993). PBLs were counted using a Bio-Rad TC20 imaging cell counter (Hercules, CA) and showed viability of ~60% by trypan blue exclusion.

For some images, HL-60 cells or PBLs were subjected to centrifugation in the Cytospin3 cytological centrifuge (Shandon Co.) at 26.6 *g* (500 rpm) for 5 min, followed by staining with the Three Step Stain (Richard-Allan Scientific, Kalamazoo, MI). Both Shandon and Richard-Allan Scientific have since been bought by Thermo Fisher (Pittsburgh, PA).

Data analysis and statistics. Error bars shown are standard deviations. Significance testing was by ANOVA using the Tukey-Kramer post-test for multiple comparisons. Significance was at $p<0.05$ unless otherwise stated.

RESULTS

To determine the possible importance of uric acid formation in the intestinal tract, we measured uric acid levels in the intestinal fluid that accumulates in response to EPEC infection at 20 h. Figure 1(A) shows the results from an experiment with rabbit EPEC strain E22 with and without erythro-hydroxynonyl adenine (EHNA), an inhibitor of the enzyme adenosine deaminase (ADA). In response to EPEC infection, the levels of uric acid increased more than 3-fold above control, to 833 μM, or 14.0 mg/dL. The uric acid level in infected loop fluid is well above the upper limit of normal for uric acid in serum (approximately 5.7 mg/dL, or 340 μM, depending on the laboratory). Addition of EHNA significantly reduced the uric acid concentration in loop fluid, suggesting that at least some

of the uric acid is derived from the breakdown of adenosine, as suggested by earlier work (Crane & Shulgina, 2009).

Since the uric acid level in loop fluids were so high, we wondered if uric acid crystals would be formed in the lumen of the gut in response to infection. We began examining the uncentrifuged, unfiltered loop fluids for evidence of birefringent crystals characteristic of uric acid. The results of examination of loop fluid using crossed polarized light is shown in Figure 1(B), with a large complex of birefringent crystals. The loop fluid in Figure 1(B) was from an intestinal segment infected with EPEC E22 and also treated with adenosine deaminase, 35 U/mL. The crystals in Figure 1(B) are 470 μm in size from top to bottom. The results of Figure 1, Panels A and B, indicated that high concentrations of uric acid were generated in vivo in response to infection, and that the uric acid levels are sufficiently high to result in the formation of uric acid crystals in the lumen of the gut in rabbit.

Uric acid is generated by the action of xanthine oxidase, a reaction which also produces hydrogen peroxide, as described by many publications including one recent one by our laboratory (Crane et al., 2013; Hancock et al., 2002; Martin et al., 2004). Hydrogen peroxide has anti-bacterial and pro-inflammatory effects of its own, but we also wished to know if uric acid had pro-inflammatory effects. We tested the effect of adding exogenous uric acid to the rabbit intestinal loops. Figure 1(C) shows that 600 μM uric acid triggered a moderate, but statistically significant increase in myeloperoxidase (MPO) activity in rabbit loop fluid. MPO is used as a marker for the influx of polymorphonuclear leukocytes into the gut lumen. Addition of the enzyme uricase alone showed no effect, but 2 U/mL uricase reversed the pro-inflammatory effect of uric acid. Figure 1(C) shows that uric acid *per se* can have inflammatory effects in the gut, independent of H_2O_2.

To further investigate the possible leukocyte chemoattractant effect of uric acid, we first studied the effect of uric acid on HL-60 cells, a human promyelocytic leukemia cell line. HL-60 cells provided an abundant source of cells with which to refine our methods and test hypotheses before moving on to normal leukocytes. Figure 2 shows the effects of uric acid crystals on HL-60 cells, using uric acid generated from hypoxanthine plus XO as described in the Methods section. Figure 2, Panels A-C show the same microscope field. In Figure 2(A), a uric acid crystal is visible under polarized light, 165 μm in length. Figure 2(B) shows the same field by phase contrast microscopy. The uric acid crystal is barely visible as a faint shadow, with two HL-60 cells adhering to it. In the Inset to Figure 2(A), at higher magnification, the same two cells show apoptotic blebbing of their membrane surface. Figure 2(C) shows the merged image generated from the images in Panels A and B, showing that HL-60 cells appear to adhere to the surface of uric acid crystals.

Initially we thought that uric acid crystals would only be visible in unstained preparations, such as by fresh wet mount examination. Figure 2, Panels D-G, however, show that uric acid crystals could even be seen in cells prepared by Cytospin cytological centrifuge, and stained with standard histological stains, and allowed to dry. Figure 2, Panels D and E represent the same microscope field, as do Panels F and G. Figure 2(D) shows a uric acid crystal under polarized light, and Figure 2(E) shows that this crystal is completely surrounded by HL-60 cells. Figure 2(F) shows a field with at least 5 uric acid crystals, and all of them are surrounded by HL-60 cells. The largest uric acid crystals were visible on brightfield examination (e.g., Figure 2(G), large vertically oriented crystal in the center of the field), but the smaller uric acid crystals were surprisingly inconspicuous on brightfield examination, and would have been ignored as proteinaceous or non-specific debris were it not for the polarization microscopy images accompanying them. Although our results were qualitative, the clustering of HL-60 cells around uric acid crystals was striking enough to suggest that uric acid crystals trigger adherence by the leukemia cells.

The results in Figure 2 were subject to two important caveats, however. First, the adherence of HL-60 cells to the uric acid crystals might reflect their malignant phenotype and not be typical of normal, non-cancerous cells. Second, using XO to generate uric acid crystals also produces H_2O_2, and the peroxide might activate or sensitize the HL-60 cells and trigger adherence. To address these limitations we continued our studies using normal peripheral blood leukocytes, and by adding catalase and uricase as additional controls.

Peripheral blood leukocytes freshly isolated from rabbit adhered to uric acid crystals in a manner similar to the HL-60 cells, as shown in Figure 3(A). The assemblage of cells adhering to the uric acid crystal included polymorphonuclear leukocytes, which in rabbit are called heterophils, and which show eosinophilic (red) granules, as well as macrophages, and also probably small lymphocytes (Figure 3A). To reduce or eliminate the possible confounding effect of peroxide formation, experiments were also done in which we added 600 U/mL catalase, a concentration of enzyme sufficient to abolish peroxide's effects (Crane et al., 2013). Figure 3, Panels B and C, show the effect of catalase addition on leukocyte adherence. Figure 3(B) shows a uric acid crystal under polarized light (yellow arrow). Figure 3(C) shows the same field under brightfield conditions, again showing a large aggregate of leukocytes around the crystal. Figure 3(C) shows that addition of catalase did not abolish the adherence of PBLs to the crystals.

In fact, our impression was that catalase seemed to enhance, not reduce, adherence of PBLs to uric acid crystals. In contrast, when uricase was added (along with XO and hypoxanthine), formation of uric acid crystals was abolished as assessed by lack of birefringence under polarized light (black or blank images not shown). Instead of uric acid crystals, the specimens treated with uricase showed material staining a lavender color and which did not attract adherence of leukocytes (Figure 3D). Conclusions from the experiments of Figure 3 were that normal peripheral blood leukocytes, like HL-60 cells, adhere strongly to uric acid crystals, and that catalase did not abolish this adherence. In contrast, uricase did abolish the formation of crystals and their associated aggregates of cells (Figure 3D).

As with the HL-60 cells, we were interested in the effect of the uric acid on the morphology and appearance of the PBLs. In Figure 3(E), one of the heterophils in contact with a uric acid crystal appears to be in the process of releasing its secretory granules (pink granules indicated by the green arrow; another cell undergoing the same process is also visible in Figure 3(A) at lower power). In Figure 3(F), many of the cells adhering to a uric acid crystal appear to be unusually stretched or elongated (green arrows). In addition, one of the mononuclear cells adhering to the uric acid crystal shows nuclear fragmentation and blebbing of the cell membrane (red arrow), both consistent with a cell undergoing apoptosis, as was observed in the HL-60 cells (Figure 2B). Uric acid-induced apoptosis has been described by other investigators (Bordoni et al., 2005).

The results of Figure 3, together with those of Figure 1(C), are consistent with uric acid crystals themselves having leukocyte-attracting and pro-inflammatory effects in the gastrointestinal tract. Although apoptosis is considered non-inflammatory, other effects of uric acid crystals such as the ability to aggregate leukocytes and trigger release of secretory granules from heterophils would have to be considered pro-inflammatory. In addition, we would expect that the effects of uric acid *per se* would be additive with some of the pro-inflammatory effects of hydrogen peroxide produced via XO. In other words, both products of the XO reaction, hydrogen peroxide and uric acid, have detectable biological effects.

DISCUSSION

We and others have been interested in the protective as well as possible deleterious effects of the host enzyme xanthine oxidase (XO) in response to enteric pathogens (Crane et al., 2013; Martin et al., 2004). Xanthine oxidase is expressed at high levels in the gastrointestinal epithelium, liver, and in milk, and at lower levels in leukocytes (Lin & Shih, 1994) and other tissues. Most of the literature on XO focusses on the anti-microbial effects of the hydrogen peroxide produced by this enzyme. But within the last 8–10 years it has become increasingly clear that uric acid itself can have biological effects. Instead of being an inert waste product of purine metabolism, uric acid is a classic example of a danger associated molecular pattern (DAMP), which can work in concert with pathogen-associated molecular patterns (PAMPs) as a signal to the immune system. Unlike PAMPs, however, the effects of uric acid are independent of Toll-like receptors. Uric acid crystals can activate theNALP3 (also known as NLRP) inflammasome (Martinon, 2010; Martinon et al., 2006), activate protein kinase C (Popa-Nita et al., 2009) and can mimic the adjuvant alum in its ability to boost immune responses to antigens (Kool et al., 2008).

In this study we have shown that uric acid levels can rise markedly in the fluid that accumulates in the ileal lumen in response to infection with the classic rabbit EPEC strain E22. In Figure 1(A), uric acid concentrations in EPEC-infected intestinal fluid reached a level 2.5 times the upper limit of normal for serum. Polarized light microscopy showed formation of birefringent crystals in these and similar fluids (Figure 1B). Moreover, exogenous uric acid increased the amount of myeloperoxidase (MPO) activity measurable in the loop fluids in a manner reversible by the enzyme uricase (Figure 1C).

Uric acid crystals are able to recruit and adhere to HL-60 cells as well as normal peripheral blood leukocytes, inducing the formation of large aggregates of cells around the uric acid crystals (see especially Figures 2E and 3C). Hydrogen peroxide was not necessary for the formation of these large clumps of cells, since they persisted in the presence of catalase (Figure 3, Panels B and C). Addition of uricase, however, abolished the uric acid crystals and the aggregates of leukocytes surrounding them (Figure 3D). Our studies shown in Figures 2 and 3 were entirely qualitative in nature. We are attempting to develop quantitative methods for measuring the size of the cellular aggregates formed around the uric acid crystals, but traditional methods, including phase contrast microscopy and flow cytometry are not particularly helpful in this regard.

Uric acid crystals are almost invisible under phase contrast (Figure 2B), are not amenable to fluorescent labeling, and the light-scattering properties of these crystals can vary widely based on their variation in size and shape. Contrary to photographs in medical textbooks on gout, uric acid crystals are not always needle-like, but instead can be rectangular or irregular in shape, as shown in Figures 1-3 and in a recent review (Howard et al., 2011).

The possible role of uric acid crystals in inflammatory bowel disease or in post-infectious irritable bowel syndrome has received scant attention, although a strong theoretical rationale for this possibility has been proposed (Meylan et al., 2006). Since EPEC infection also triggers a release of ATP from host cells (Crane et al., 2002), multiple extracellular DAMPs are generated by this infection, possibly resulting in additive pro-inflammatory effects. “Gout of the gut,” or inflammation triggered by uric acid crystal formation in the lumen of the intestinal tract, may be involved in other disorders than just infection due to enteropathogenic and Shiga-toxigenic *E. coli*. Blocking formation of uric acid might be beneficial in certain inflammatory disorders of the GI tract. Conversely, adding uric acid or promoting its formation might be a way to increase the immunogenicity of oral vaccines, such as oral cholera vaccines (Clemens, 2011).

Acknowledgments

I also thank my friend Robert C. Duncan, Dept. of Astronomy, Univ. of Texas at Austin, for reminding me that calcite crystals show birefringence. Dr. Duncan shared the Bruno Rossi Prize for High-Energy Astrophysics in 2003. I (J.K.C.) thank Dr. Robert Hard, University at Buffalo, for showing me how to determine negative birefringence by the first order red plate method.

We thank the National Institutes of Health for funding via grant R21 AI 102212.

REFERENCES

Harrison R. Milk xanthine oxidase: Properties and physiological roles. Inter Dairy J. 2006; 16:546–54.

Martin H, Hancock J, Salisbury V, et al. Role of xanthine oxidoreductase as an antimicrobial agent. Infect Immun. 2004; 72:4933–9. [PubMed: 15321984]

Hancock J, Salisbury V, Ovejero-Boglione M, et al. Antimicrobial properties of milk: Dependence on presence of xanthine oxidase and nitrite. Antimicrobial Agents Chemother. 2002; 46:3308–10.

Kotloff KL, Nataro JP, Blackwelder WC, et al. Burden and aetiology of diarrhoeal disease in infants and young children in developing countries (the Global Enteric Multicenter Study, GEMS): A prospective, case-control study. Lancet. 2013; 382:209–22. [PubMed: 23680352]

Frank C, Werber D, Cramer JP, et al. Epidemic profile of shiga-toxin-producing *Escherichia coli* O104:H4 Outbreak in Germany. New Engl J Med. 2011; 365:1771–80. [PubMed: 21696328]

Bianchi ME. DAMPs, PAMPs and alarmins: All we need to know about danger. J Leuko Biol. 2007; 81:1–5. [PubMed: 17032697]

Shi Y, Evans J, Rock K. Molecular identification of a danger signal that alerts the immune system to dying cells. Nature. 2003; 425:516–21. [PubMed: 14520412]

Heath W, Carbone F. Dangerous liaisons. Nature. 2003; 425:460–1. [PubMed: 14523425]

Behrens MD, Wagner WM, Krco CJ, et al. The endogenous danger signal, crystalline uric acid, signals for enhanced antibody immunity. Blood. 2008; 111:1472–9. [PubMed: 18029553]

Howard SC, Jones DP, Pui C-H. The Tumor Lysis Syndrome. New Engl J Med. 2011; 364:1844–54. [PubMed: 21561350]

Crane J, Naeher T, Shulgina I, et al. Effect of zinc in enteropathogenic Escherichia coli infection. Infect Immun. 2007; 75:5974–84. [PubMed: 17875638]

Milon A, Oswald E, De Rycke J. Rabbit EPEC: A model for the study of enteropathogenic *Escherichia coli*. Veter Res. 1999; 30:203–19.

Crane JK, Naeher TM, Broome JE, et al. Role of host xanthine oxidase in infection due to enteropathogenic and shiga-toxigenic *Escherichia coli*. Infect Immun. 2013; 81:1129–39. [PubMed: 23340314]

Crane JK, Majumdar S, Pickhardt DP. Host cell death due to enteropathogenic Escherichia coli has features of apoptosis. Infect Immun. 1999; 67:2575–84. [PubMed: 10225923]

Tait AR, Davidson BA, Johnson KJ, et al. Halothane inhibits the intraalveolar recruitment of neutrophils, lymphocytes, and macrophages in response to influenza virus infection in mice. Anesthes Analges. 1993; 76:1106–13.

Crane JK, Shulgina I. Feedback effects of host-derived adenosine on enteropathogenic *Escherichia coli*. FEMS Immunol Med Microbiol. 2009; 57:214–28. [PubMed: 19751218]

Bordoni V, De Cal M, Rassu M, et al. Protective effect of urate oxidase on uric acid induced-monocyte apoptosis. Curr Drug Discov Technol. 2005; 2:29–36. [PubMed: 16472239]

Lin J-K, Shih C-A. Inhibitory effect of curcumin on xanthine dehydrogenase/oxidase induced by phorbol-12-myristate-13-acetate in NJH3T3 cells. Carcinogenesis. 1994; 15:1717–21. [PubMed: 8055654]

Martinon F, Petrilli V, Mayor A, et al. Gout-associated uric acid crystals activate the NALP3 inflammasome. Nature. 2006; 440:237–41. [PubMed: 16407889]

Martinon F. Mechanisms of uric acid crystal-mediated autoinflammation. Immunol Rev. 2010; 233:218–32. [PubMed: 20193002]

Popa-Nita O, Proulx S, Pare G, et al. Crystal-induced neutrophil activation: XI. Implication and novel roles of classical protein kinase C. J Immunol. 2009; 183:2104–14. [PubMed: 19596988]

Kool M, Soullie T, van Nimwegen M, et al. Alum adjuvant boosts adaptive immunity by inducing uric acid and activating inflammatory dendritic cells. J Exper Med. 2008; 205:869–82. [PubMed: 18362170]

Meylan E, Tschopp J, Karin M. Intracellular pattern recognition receptors in the host response. Nature. 2006; 442:39–44. [PubMed: 16823444]

Crane J, Olson R, Jones H, et al. Release of ATP during host cell killing by enteropathogenic E. coli and its role as a secretory mediator. Am J Physiol (Gastrointest Liver Physiol). 2002; 282:G74–86. [PubMed: 12065294]

Clemens JD. Vaccines in the time of cholera. Proc Natl Acad Sci. 2011; 108(85):29–30. [PubMed: 21149685]

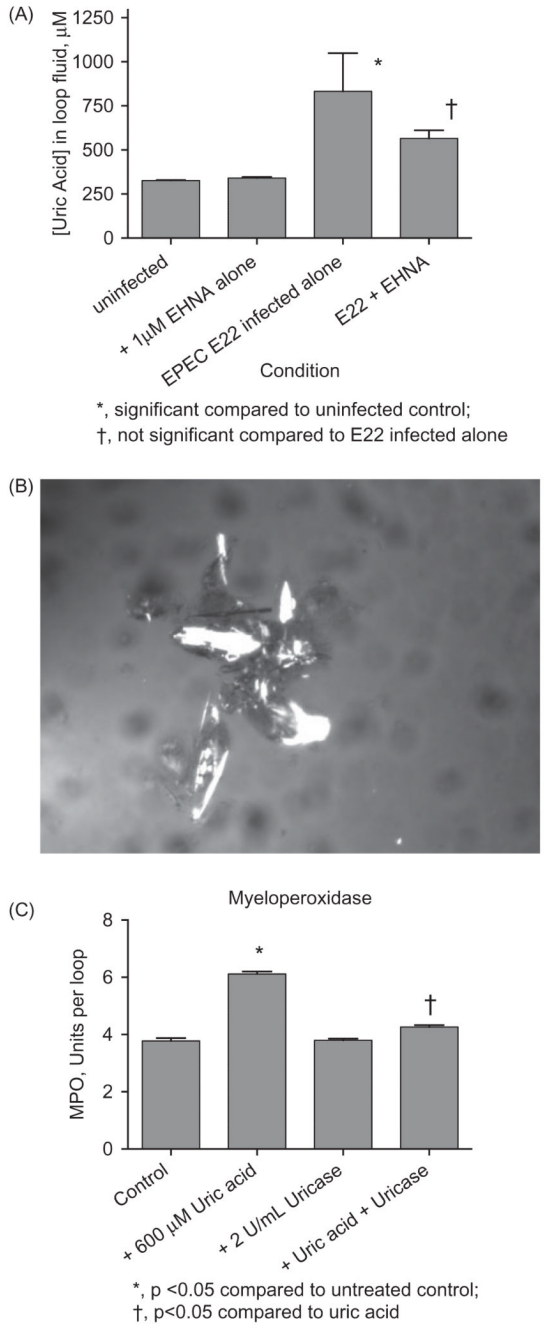

Figure 1.

Formation of uric acid in vivo in rabbit intestinal loops in response to EPEC infection. Panel A. Uric acid levels were measured in the fluid that accumulates in the intestinal loops following infection with rabbit EPEC strain E22 at 20 h after infection, with and without 1 μM EHNA, an adenosine deaminase (ADA) inhibitor. Panel B, microscopic evidence for uric acid crystal formation in the unfiltered loop fluid of a rabbit infected with E22 with 35 U/mL ADA. The large group of birefringent crystals was 470 μm in size in the vertical dimension. Panel C, pro-inflammatory effects of exogenous uric acid in vivo in rabbit intestinal loops. No pathogenic bacteria were added in the experiment shown in Panel C, but instead uric acid, uricase, or the combination of the two was added. Loop fluid was analyzed

for MPO activity. Panel C is from Gut Microbes 4; 5; 1–4, 2013, http://dx.doi.org/10.4161/gmic.25584, under the provisions of the Creative Commons Attribution License.

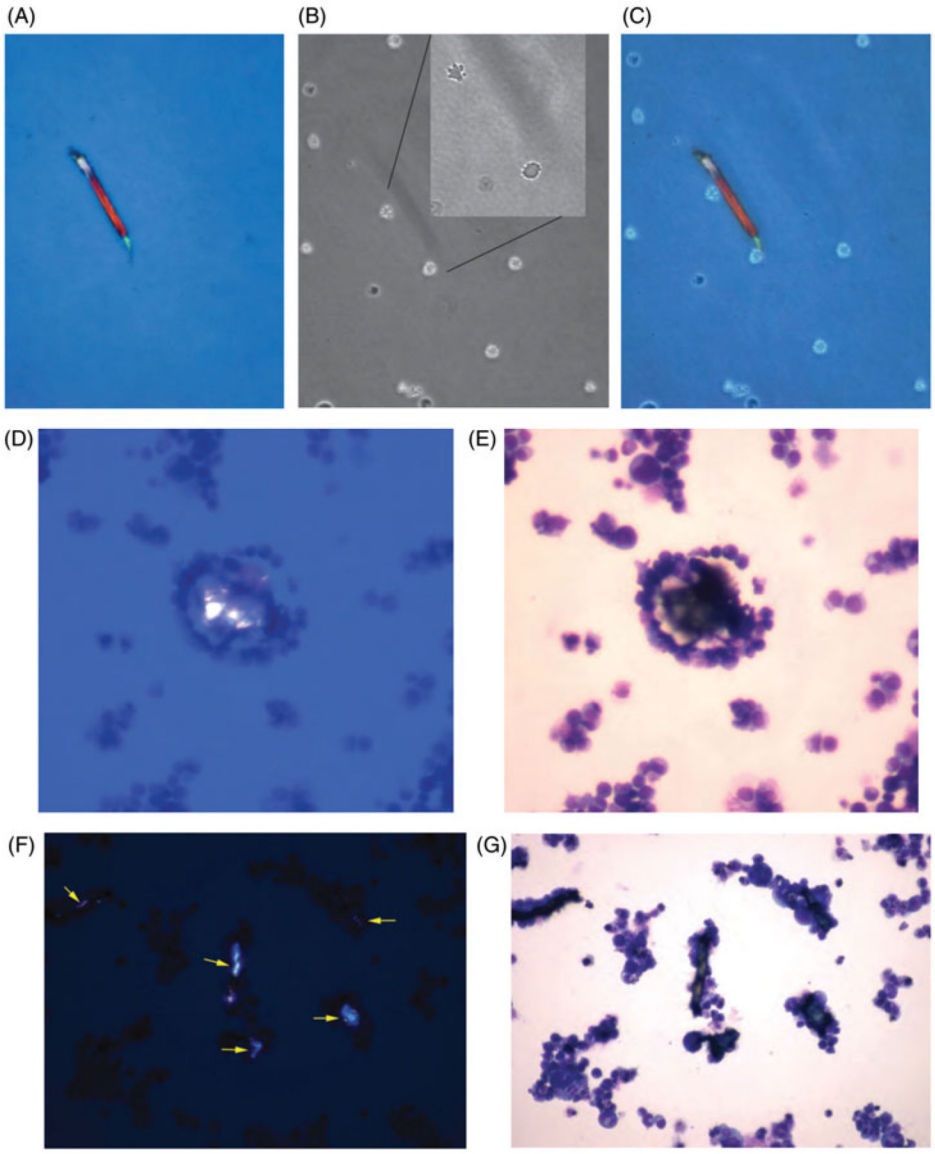

Figure 2.

Interactions between uric acid crystals and HL-60 leukemia cells. Uric acid was generated enzymatically by adding 400 μM hypoxanthine and 0.5 U/mL XO to suspensions of HL-60 cells and incubating at 37 °C in 5% CO2 for 1.5 h. Then the HL-60 cells were examined using a wet mount preparation and cover slip (Panels A-C) or by concentration in the Cytospin centrifuge followed by staining (Panels D-G). Panel A, polarization microscopy showing a birefringent crystal 165 μm in length. Panel B, same field examined by phase contrast, showing two cells associated with the crystal. Panel B, Inset, higher power view showing blebbing of the cell surface of the two adherent HL-60 cells. Panel C, merged image of Panels A and B. Panels D and E show the same field examined using two different methods of illumination; polarization in Panel D and brightfield in Panel E, showing tight clustering of HL-60 cells around the uric acid crystal. Panels F and G again show a pair of images of the same microscope field, with Panel F showing at least 5 birefringent crystals. On brightfield examination, all of the crystals are covered by a tight layer of adhering cells. Note that only the largest crystal (center) is visible by brightfield exam alone.

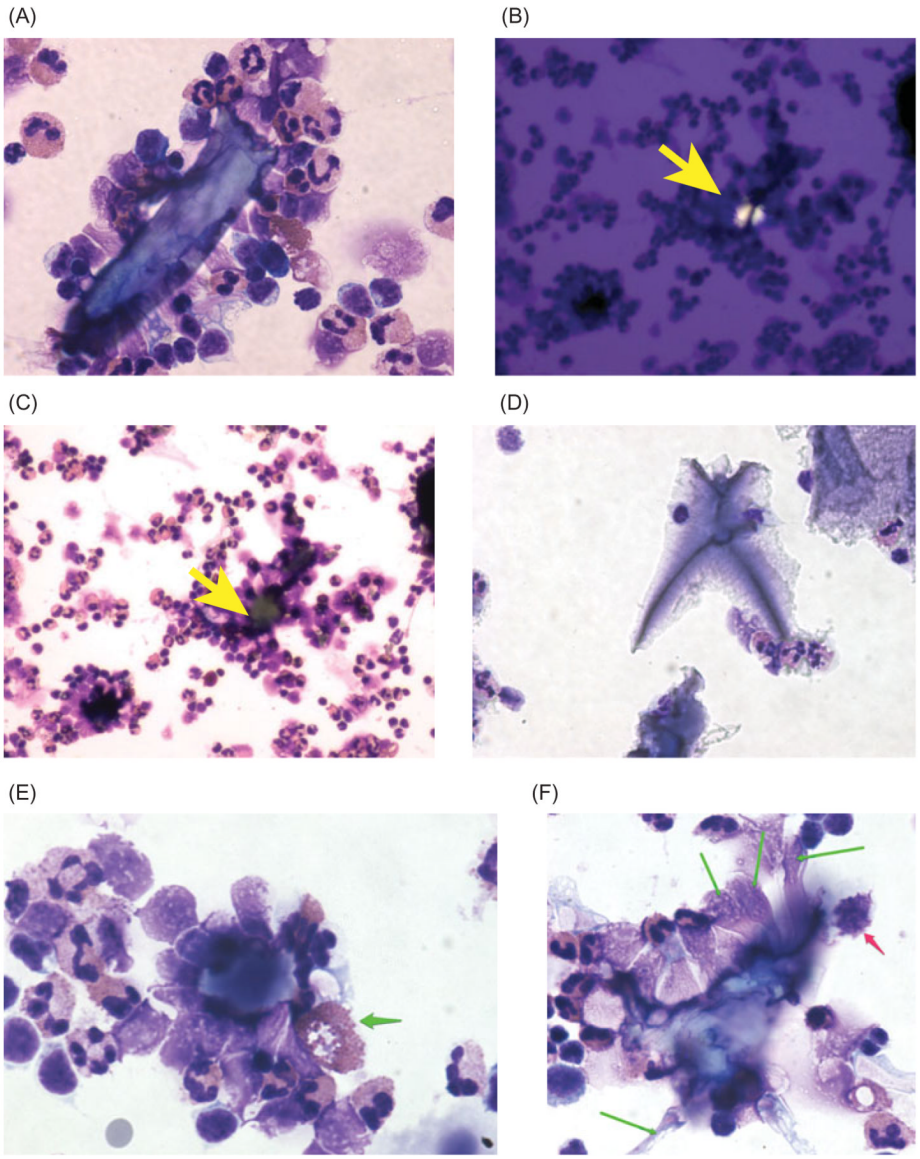

Figure 3.

Interactions between uric acid crystals and rabbit peripheral blood leukocytes (PBLs). Uric acid was again generated by addition of 400 μM hypoxanthine +0.5 U/mL XO to suspensions of freshly isolated PBLs for 1.5 h, followed by Cytospin centrifugation and staining. In some conditions (Panels B and C), 600 U/mL catalase was added to break down hydrogen peroxide, while in others 2 U/mL uricase was added to remove uric acid by conversion to allantoin. Panel A, large cluster of PBLs surrounding a uric acid crystal 85 μm in length; original magnification, 400×. Panels B and C, a pair of images showing a uric acid crystal (Panel B, yellow arrow) completely surrounded by a large aggregate of PBLs (Panel C), where the yellow arrow again indicates the location of the crystal, which appears as a non-descript piece of debris on brightfield examination. Panel D, addition of uricase abolished the formation of crystals and also the aggregates of PBLs. Panel E, heterophil adhering to a uric acid crystal and showing release of its secretory granules (green arrow). Panel F, PBLs adhering to a uric acid crystals show elongation (green arrows), and a

mononuclear cell shows signs of apoptosis (red arrow); original magnification of Panels E and F, 600 X.